Genesis of Si-rich carbonatites in Huanglongpu Mo deposit, Lesser Qinling orogen, China and significance for Mo mineralization

CrossMark

Wenlei Song [a], Cheng Xu [a,*], Liang Qi [b], Li Zhou [b], Linjun Wang [c], Jindrich Kynicky [d]

[a] Laboratory of Orogenic Belts and Crustal Evolution, School of Earth and Space Sciences, Peking University, Beijing 100871, China
[b] Laboratory for High Temperature & High Pressure Study of the Earth's Interior, Institute of Geochemistry, Chinese Academy of Sciences, Guiyang 550002, China
[c] Engineering Research Center for Geologic Hazards Prevention, Guizhou Minzu University, Guiyang 550025, China
[d] Department of Geology and Pedology, Mendel University of Agriculture and Forestry, Brno, Czech Republic

ABSTRACT

The Huanglongpu carbonatite-related Mo ore field is located in the Lesser Qinling Orogenic belt in the southern margin of the North China block. The ore field is composed of six deposits, Yuantou, Wengongling, Dashigou, Shijiawan, Taoyuan and Erdaohe, all of which are genetically related to carbonatite dykes except for the Shijiawan deposit which is associated with a granitic porphyry. The Yuantou carbonatite dykes intruded into Archean gneiss and other carbonatites emplaced into Mesoproterozoic volcanic and sediment rocks. The carbonatites are mainly composed of calcite and variable amounts of quartz and K-feldspar and minor molybdenite. Re–Os dating of molybdenite from the Yuantou carbonatite yields a weighted average age of 225.0 ± 7.6 Ma, consistent with the molybdenite age (221 Ma) from the Dashigou deposit. The rocks are characterized by high heavy REE (HREE) contents and consistent flat REE distribution patterns with La/Yb$_{cn}$ ~1. Quartz in the carbonatites from Yuantou and Dashigou deposits shows consistent O isotopes (8.1–10.2‰) similar to the associated calcite (7.2–9.5‰). The quartz and associated K-feldspar contain lower Zr, Hf and higher HREE abundances and negligible Eu anomaly relative to those from the granite porphyry in Shijiawan. Both minerals are primary products in the carbonatitic liquid, and not captured from the wall-rocks or crustal-derived silicate magmas, or a hydrothermal origin. Thus, the Huanglongpu carbonatitic liquids were enriched in Si and Mo, which may be produced by intensely fractional crystallization of non-silicate minerals.

© 2014 Elsevier B.V. All rights reserved.

1. Introduction

Carbonatites are defined as igneous rocks composed of more than 50 modal percent carbonate and containing less than 20 wt.% SiO_2 (Le Maitre, 2002). They are characterized by high concentrations of Sr and rare earth elements (REE) (Hornig-Kjarsgaard, 1998; Woolley and Kempe, 1989; Xu et al., 2008, 2010). Many rare metal and non-metal ores including Nb, REE, fluorite and phosphate come from carbonatites, and minerals such as baddeleyite and vermiculite frequently occur in silicate rocks associated with carbonatites (Mariano, 1989). However, sulfide deposits are quite uncommon in carbonatites and associated alkaline silicate rocks. Only several places, to the best of our knowledge, have been reported to possess sulfide mineralization including the super-large copper deposit within the Phalaborwa carbonatites, South Africa (Eriksson, 1989; Heinrich, 1970; Palabora Mining Company, 1976), sub-economic copper mineralization within the Kovdor phoscrorite–carbonatite (Rudashevsky et al., 2001) and melteigite–

ijolite in Salmagorskii carbonatite complex, Russia (Korobeinikov et al., 1998).

Carbonatites generally contain minor primary silicate minerals such as olivine, clinopyroxene, mica, amphibole and titanite (Gitins et al., 2005; Horgarth, 1989). Experimental studies also show that carbonatitic liquids may precipitate silicate minerals (e.g., Dalton and Presnall, 1998; Wallace and Green, 1988). However, feldspar and quartz in many carbonatites have been considered as xenocrysts or products of subsolidus alteration (Barker, 2001; Le Bas, 1989), representing an altered composition rather than primary phases precipitated from carbonatitic melts.

The cabonatites from Huanglongpu in northmost Qinling (commonly referred to as "the Lesser Qingling"), China, are unusual in that they contain abundant (0.18 million t) Mo metals and formed a large Mo deposit (Xu et al., 2010). The Qinling area is the largest Mo mineralization belt in the world. The majority of these deposits are hosted by granitic porphyry and transitional porphyry–skarn (Li et al., 2007; Mao et al., 2008). The carbonatite-type Mo deposit is rare and only found in China until now. The Huanglongpu ore field is composed of six deposits: Yuantou, Wengongling, Dashigou, Shijiawan, Taoyuan and Erdaohe, and occurs in various host-rocks including Archean gneiss and

* Corresponding author. Tel./fax: +86 10 6275 1187.
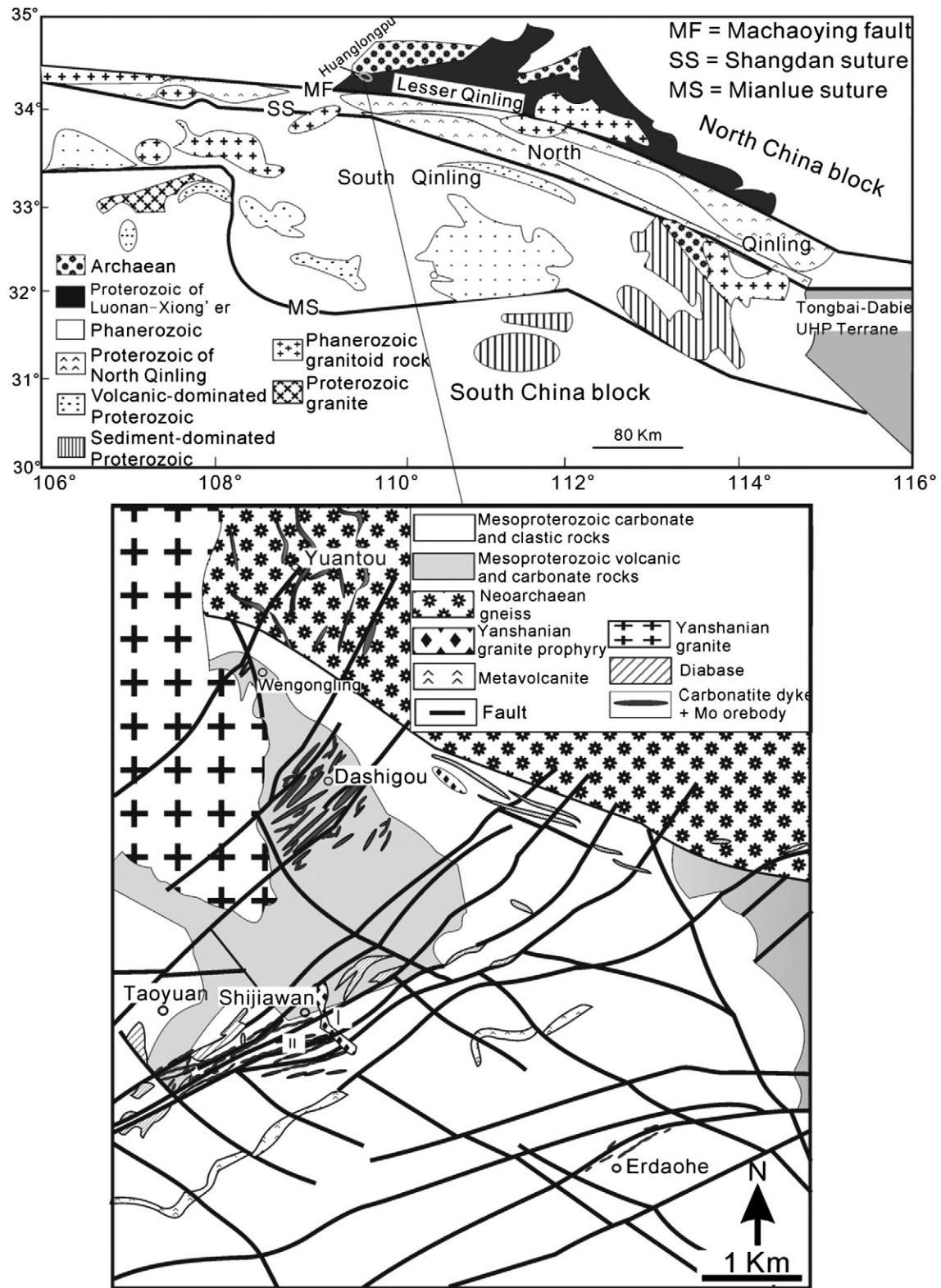 E-mail address: xucheng1999@hotmail.com (C. Xu).

Fig. 1. Geological sketch of the Hunaglongpu deposit (modified after Xu et al., 2010).

Mesoproterozoic volcanic and sediment rocks. The mineralization in Shijiawan is a granite porphyry–Mo system different from other orefields. It is not clear whether Mo mineralization is coeval or represents different stages because only a molybdenite age from Dashigou in Mesoproterozoic groups has been previously reported (Huang et al., 1994). Additionally, the geochemical features of carbonatites from

Wenggongling and Yuantou deposits in different wall-rocks were not previously reported. The carbonatites contain variable amounts of K-feldspar (up to 5%) and quartz (up to 15%). Both minerals are also common in granite porphyry deposits, and their origin in the carbonatites and potential relationship with Mo mineralization are not known. In this study, carbonatite samples from Yuantou, Dashigou and Taoyuan
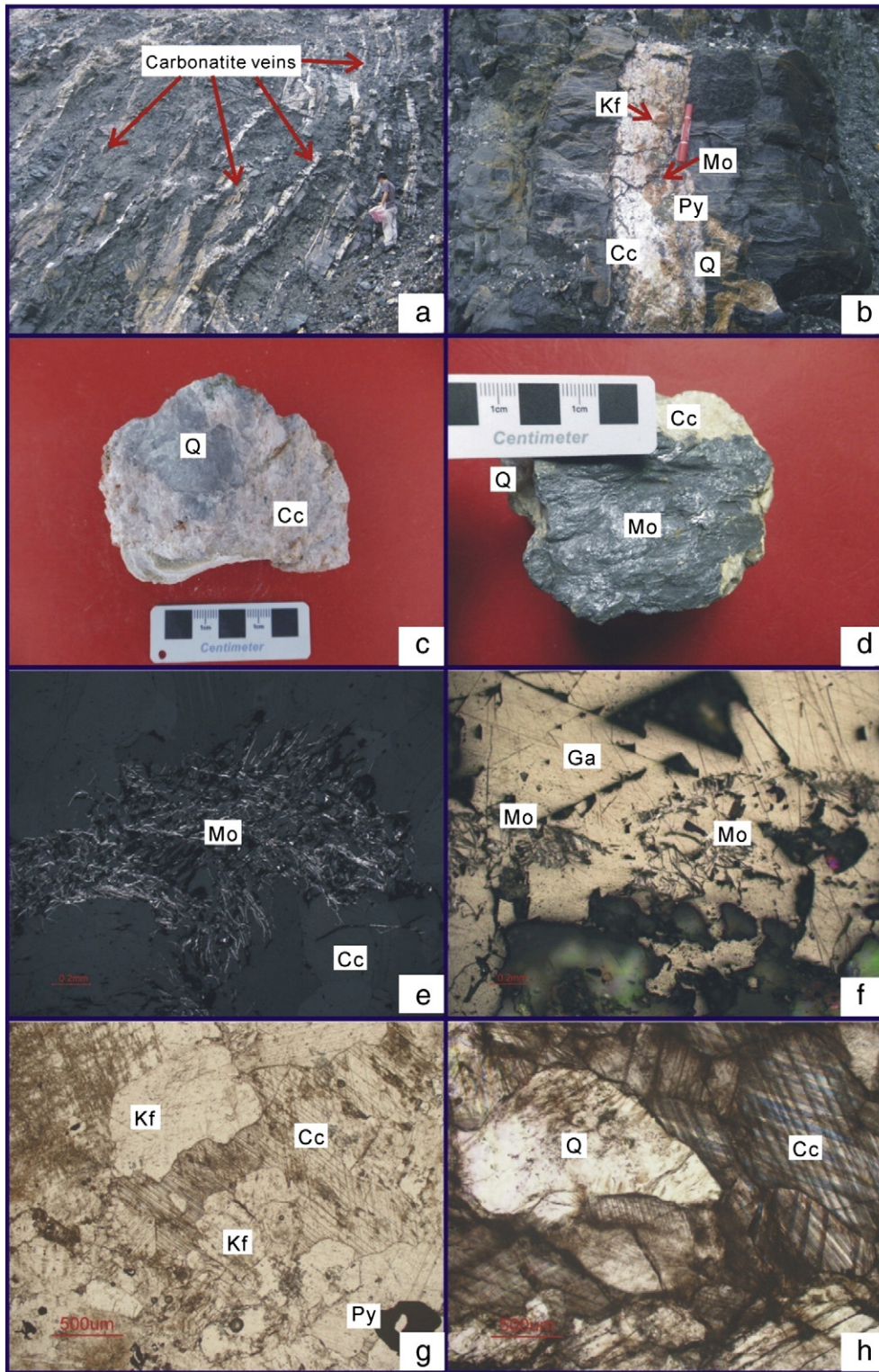
Fig. 2. Photographs showing ore petrography of the Huanglongpu deposit. (a): Carbonatites form as clusters of dyke ranging from several tens of centimeters to less than 1 meter in thickness at Dashigou orefield. (b): Individual carbonatite dyke consisting of calcite, quartz, K-feldspar, pyrite and molybdenite. (c): Quartz occurring as massive-shaped aggregation in the carbonatite dyke. (d): Molybdenite occurring as thin films at the contact between the carbonatite and wall-rock. (e) and (f): Molybdenite occurring as infillings along calcite or galena cleavage planes. (g) and (h): K-feldspar and quartz occurring as euhedral–subhedral phenocryst and allotriomorphic granule, respectively, in a fine-grained matrix of calcite. Cc, calcite; Kf, K-feldspar; Mo, molybdenite; Py, pyrite; Ga, galena; Q, quartz.

were collected. Re–Os dating of molybdenite and geochemical analyses of quartz and K-feldspar in the carbonatites were carried out, and quartz and K-feldspar from porphyry granite in Shijiawan were compared in order to study the genesis of the carbonatites and their hosting Mo mineralization.

2. Geology

The Huanglongpu Mo district is located in the Lesser Qinling orogenic belt, which extends from the eastern Shanxi Province to the southern Henan Province of China along the southern margin of the

Table 1
Re–Os values of molybdenites from Huanglongpu deposit.

Sample no.	Mine	Re(ppm)	^{187}Re(ppm)	^{187}Os(ppb)	Model age (Ma)	References
HD80-1	Dashigou	283.50 ± 6.9	177.5 ± 4.3	669.5 ± 13.1	230 ± 7	Huang et al. (1994)
HD81-96		256.00 ± 3.5	160.3 ± 2.2	583.9 ± 20.7	222 ± 8	
HD81-101		438.60 ± 6	274.6 ± 3.7	1024 ± 25	227 ± 7	
HD93-10		530.60 ± 12.9	332.1 ± 8.1	1261.6 ± 24.8	231 ± 7	
HD93-11		633.10 ± 5.4	396.3 ± 3.4	1431.1 ± 30.3	220 ± 5	
HLP-5		278.10 ± 0.5		645 ± 2	221.1 ± 0.9	Stein et al. (1997)
HLP-5		285.30 ± 0.5		662 ± 2	221.1 ± 0.9	
HLP-5		289.10 ± 0.5		672 ± 2	221.6 ± 0.9	
HLP-5		281.80 ± 0.5		656 ± 2	221.9 ± 0.9	
HLP-5		284.40 ± 0.5		662 ± 2	222 ± 0.9	
HLP-5		282.70 ± 0.5		657 ± 2	221.5 ± 0.9	
HLP-5		284.50 ± 0.5		661 ± 2	221.5 ± 0.9	
YT-1-1	Yuantou	236.8 ± 9	148.2 ± 5.6	542.6 ± 9.8	220.1 ± 4.0	This study
YT-2-1		250.3 ± 6.4	156.7 ± 4.0	605.5 ± 10.6	232.3 ± 4.0	
YT-3-1		225.9 ± 6.5	141.4 ± 4.1	515.4 ± 10.5	219.2 ± 4.5	
YT-6-2		301.4 ± 12.1	188.7 ± 7.6	721.5 ± 12.3	229.9 ± 3.9	
YT-7-1		260.5 ± 22.7	163.1 ± 14.2	619.4 ± 10.5	228.4 ± 3.9	
YT-8-1		159.4 ± 8.7	99.8 ± 5.5	358.0 ± 9.5	215.8 ± 5.8	

Note: Calculated with the equation: t = In (1/λ)(1 + 187Os/187Re), where λ is the decay constant of ^{187}Re, 1.64 × 10^{-11}/a (Lindner et al., 1989).

North China block. The Qinling orogen is composed of South Qinling, North Qinling and Lesser Qinling separated by major faults (Fig. 1). The North Qinling belt is regarded as a Mid-Paleozoic orogen with widespread Paleozoic island-arc type magmatism and metamorphism (Sun et al., 2002). The South Qinling belt is interpreted as a Late-Paleozoic to Early-Mesozoic orogen characterized by abundant Triassic granitic magmatism and metamorphism (Mattauer et al., 1985; Sun et al., 2000). The Lesser and North Qinling areas include five world-class superlarge (>5 × 10^5 t Mo), five large (5–20 × 10^4 t Mo) and several medium and small (<5 × 10^4 t Mo) deposits (Li et al., 2007; Mao et al., 2008). Most of them are hosted by granitic porphyry. Detailed descriptions of the geological framework and tectonic evolution of the Qinling region are given in Meng and Zhang (2000), Ratschbacher et al. (2003) and Xu et al. (2011).

The Huanglongpu area is composed of the Mesoarchean (2806–2841 Ma; Kröner et al., 1988) Taihua high-grade Group, which is uncomformably overlain by the Mesoproterozoic (ca. 1780–1770 Ma) Xiong'er Group consisting of alkaline, bimodal, basaltic-andesite and dacite. NW- to WNW-trending detachment fault structures were widely developed in the region (Mao et al., 2008). Granite porphyry (zircon U–Pb age of 141 Ma, Zhao et al., 2010a), alkaline granite porphyry (zircon U–Pb age of 131 Ma; Zhao et al., 2010b) and diabase (zircon U–Pb age of 129 Ma; Zhao et al., 2010b) outcrop sporadically. The carbonatites occur as dykes and discontinuously extend about 6 km, mainly controlled by the above fault zone. The district is composed of six deposits at Yuantou,
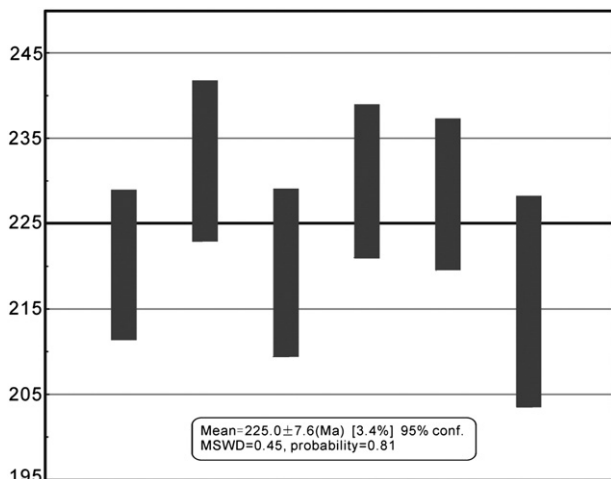
Wengongling, Dashigou, Shijiawan, Taoyuan and Erdaohe from north to south (Fig. 1). Besides carbonatites, the granite porphyry at Shjiawan also contains abundant molybdenite.

The Yuantou carbonatites intruded into Neoarchean Taihua gneiss, and the other carbonatites in Huanglongpu ore field into the Mesoproterozoic volcanic, carbonate and clastic rocks. Individual carbonatite dykes range from several tens to hundreds of meters in length and <1 m in thickness (Fig. 2a, b). They consist of calcite (>80%), quartz (<15%), barite (<5%), K-feldspar (<5%), pyrite, galena, sphalerite, molybdenite, biotite, REE-fluorocarbonates, monazite and brannerite. Calcite usually occurs as coarse pink clusters (Fig. 2b, c). Quartz is the second most (up to 15% in volume) common mineral and mostly occurs as massive (Fig. 2c, h) aggregates. K-feldspar is a modally significant constituent of the carbonatites (up to 5% in volume), and usually occurs as euhedral phenocryst aggregates (Fig. 2b) with a composition range Or$_{81-97}$Ab$_{2-18}$An$_{0-0.1}$ (Xu et al., 2010). Molybdenite occurs as variety of forms in the carbonatite dyke: thin films at the contact between the carbonatite and wall-rock (Fig. 2d), disseminated aggregates (Fig. 2b), and infillings along calcite or galena cleavage planes (Fig. 2e and f). In the Shijiawa porphyry deposit, the granite consists of K-feldspar (50–60%), quartz (20–40%) and plagioclase (10–25%), which intruded the Mesoproterozoic volcanic, carbonate and clastic rocks. The ore assemblages of quartz–pyrite–molybdenite and quartz–K-feldspar–molybdenite are observed in a roof pendant composed of porphyry. Presently, Dashigou is under open-pit mining (Fig. 2a), and other carbonatite orefields are mined underground. The granite porphyry Mo deposit in Shijiawa has both open-pit and underground mining. According to the report of No. 13 Geological Team (1989), both Dashigou and Shijiawa are large Mo deposits, with current reserves of 8.9 × 10^4 and 8 × 10^4 t and a grade of 0.075–0.103% and 0.071% (average) Mo, respectively; Taoyuan orebody has reserves of 3.8 × 10^4 t of Mo with a grade of 0.041–0.096% Mo; Yuantou, Wengonling and Erdaohe orebodies have ore grades of 0.07–0.114%, 0.036–0.136% and 0.034–0.129% Mo, and their real reserves are not presently reported. Re–Os dating of molybdenite from the Dashigou carbonatites and Shijiawa granite porphyry yields ages of 221.1 ± 0.9 Ma (Stein et al., 1997) and 140.4 ± 2–140.9 ± 2 Ma (Mao et al., 2008), respectively. The granite porphyry has a zircon U–Pb age of 141.4 ± 0.6 Ma (Zhao et al., 2010a). The age of the Yuantou

Fig. 3. Weighted average plots of molybdenite Re–Os data from Yuantou orefield.

Mean=225.0±7.6(Ma) [3.4%] 95% conf.
MSWD=0.45, probability=0.81

Table 2
Result of the analysis of oxygen isotope in quartz form Huanglongpu deposit.

Sample no.	YT-1	YT-2	DSG-1	DSG-2	DSG-5
σ^{18}O(‰,SMOW)	9.8	8.8	8.5	8.1	10.2

Table 3
Trace element contents (ppm) of carbonatite, K-feldspar and quartz in Huanglongpu deposit.

Samples	Carbonatite													
	YT-1	YT-2	YT-3	YT-4	YT-5	YT-6	YT-7	YT-8	YT-9	WGL-1	WGL-2	WGL-3	WGL-4	DSG-1
Rb	0.33	0.41	0.63	0.29	0.31	0.33	0.28	0.25	0.18	0.28	0.77	0.23	0.24	0.22
Ba	372	724	267	99.0	165	201	738	418	212	141	302	2919	134	551
Th	0.44	0.25	0.68	0.11	0.27	0.36	0.41	0.22	0.23	0.28	0.45	1.32	0.54	0.46
U	0.31	0.25	0.54	0.12	0.63	0.18	0.46	0.40	0.59	0.42	5.81	2.79	0.38	0.75
Nb	0.34	0.12	0.47	0.07	0.57	0.12	0.32	0.64	0.38	0.18	0.39	1.39	0.29	0.39
Ta	0.21	0.21	0.17	0.18	0.15	0.16	0.17	0.16	0.13	0.13	0.09	0.08	0.11	0.11
Mo	0.79	1.16	6.03	63.8	4.35	3.02	1.07	2.21	1.44	0.55	4.57	5.73	1.37	1.37
La	149	127	168	226	129	129	128	105	181	452	306	282	509	230
Ce	379	340	414	612	312	328	313	268	402	1106	763	659	1260	595
Pb	105	118	111	133	107	125	162	123	120	113	116	103	132	96.0
Pr	50.7	48.0	53.1	81.6	40.0	43.0	41.9	35.6	49.3	129	97.1	84.8	149	78.1
Sr	6607	6323	6324	7068	4747	5997	5466	4840	4585	7181	4368	7872	7258	6084
Nd	239	239	240	373	179	204	201	170	218	539	425	374	612	351
Sm	63.8	72.2	63.0	90.5	50.3	58.0	59.0	49.5	54.8	95.8	85.1	78.2	109	82.5
Zr	0.28	0.11	0.31	0.34	0.17	0.31	0.33	0.22	0.30	0.23	0.32	0.18	0.40	0.37
Hf	0.97	1.17	0.95	1.27	0.90	0.90	0.88	0.80	0.78	0.86	0.53	0.35	0.71	0.56
Eu	21.2	24.0	20.0	27.9	16.1	19.5	19.7	16.8	17.7	27.4	23.9	21.9	31.1	24.6
Gd	88.5	108	88.3	112	73.1	86.6	86.3	77.7	77.0	103	79.4	72.3	109	89.2
Tb	12.1	14.6	11.4	14.2	10.2	12.1	12.6	11.2	10.7	12.8	9.80	8.90	14.6	12.2
Dy	81.6	102	75.8	88.2	70.7	82.2	90.0	80.9	76.3	80.1	54.7	49.6	90.1	76
Y	680	857	594	648	563	714	699	642	559	622	314	269	646	513
Ho	18.9	24.6	16.9	18.8	17.2	20.0	22.4	20.7	18.8	19.0	11.3	10.1	21.7	16.5
Er	63.2	81.4	56.4	60.0	60.1	67.2	76.4	73.2	64.6	65.0	33.4	30.8	73.6	51.3
Tm	11.0	14.6	9.35	9.74	10.8	11.8	13.8	13.4	11.6	11.0	5.06	4.84	12.4	8.31
Yb	77.5	106	66.4	69.9	82.2	85.3	107	103	89.0	80.1	35.8	33.1	90.5	56.6
Lu	11.1	16.7	9.66	10.5	13.5	12.6	17.2	16.8	14.8	12.0	5.05	4.87	13.1	8.19

carbonatites is unknown. In this study, carbonatite samples from Yuantou, Wengongling, Dashigou and Taoyuan were collected. For comparison, molybdenite from Yuantou carbonatites, and quartz and K-feldspar from the Shijiawan granite porphyry were also collected.

3. Analytical methods

The molybdenites sampled from Yuantou carbonatite veins were used for Re–Os dating and the purity of the mineral can reach to 99% after separation and selection. All samples prepared for trace element analysis were from the fresh mineral aggregates with well formed idiomorphic crystal. The samples were crushed down to 1 mm sieved and washed, then handpicked carefully under a binocular microscope again. It's a necessity that the K-feldspar and quartz were leached with dilute acetic acid to remove mainly carbonate dust avoiding contamination. Finally, the obtained mineral grains were cleaned using an ultrasonic water bath. Some of the quartz separates were taken for analysis of oxygen isotope and the other mineral separates ground to powder in an agate mill.

Re–Os isotope analysis of molybdenite from the Yuantou carbonatites was carried out on an ELAN DRC-e Quadropole ICP-MS at the Institute of Geochemistry of the Chinese Academy of Sciences. Molybdenites were first digested with HNO_3 in a 120 ml Carius tube. The released additional gas and a small portion of volatile Os were collected by 10 mol/l of HCl in an ice-water bath. After the sulfides were totally reacted with HNO_3, the HCl solution containing all the released Os was transferred back to the Carius tube. The sample was further digested in aqua regia at 200 °C for about 10 h in a sealed Carius tube. Osmium was separated from the matrix by distillation and Re by anion exchange resin. The instrument sensitivity was greater than 40000 cps for 1 ng/ml of ^{115}In, and the relative standard deviation (RSD%) was less than 3%. Detailed analytical procedures, including chemical separation of Rhenium and Osmium and mass spectrometric determination, are described by Qi et al. (2010).

Trace elements of the carbonatites and mineral separates were determined by a Quadropole ICP-MS at the Institute of Geochemistry

of the Chinese Academy of Sciences. Prior to the analysis, 50 mg of rock powder were dissolved in a Teflon bomb using 1 ml of HF (38%) and 0.5 ml of HNO_3 (68%). The sealed bomb was placed in an electric oven and heated to 180 °C for 24 h. The cooling solution was added 1 ml of 1 μ gml^{-1} Rh as internal standard and evaporated on the hot plate. This was followed by two cycles of dilution with 1 ml of HNO_3 and evaporation to dryness. The final residue was re-dissolved in 8 ml of HNO_3. The bomb was re-sealed, returned to the oven and heated to 135 °C for 5 h. The final solution was diluted to 100 ml by the addition of distilled de-ionized water for ICP-MS analysis. The analytical precision for most elements is generally better than 10%. Further details of this analysis are given in Qi et al. (2000).

Oxygen isotope of the quartz was analyzed at the Institute of Mineral Resources of the Chinese Academy of Geological Sciences. Quartz was dried in vacuum oven under the temperature of 105 – 110 °C and then weight of about 12 mg of sample reacted with BrF_5 at high temperature between 500 °C and 550 °C. The released oxygen is converted to CO_2 by reaction with hot carbon in the presence of a Pt-catalyst. The CO_2 was admitted on-line to the MAT253 mass spectrometer. The analytical precision of the instrument is ± 0.2‰. The results are reported with the notation relative to standard mean ocean water (SMOW):

$$\delta^{18}O = \left[\left({}^{18}O/{}^{16}O \right)_{sample} \Big/ \left({}^{18}O/{}^{16}O \right)_{SMOW} - 1 \right] \times 1000\text{‰}.$$

4. Results

4.1. Re–Os age

Re–Os analyses of six molybdenites from the Yuantou carbonatite are listed in Table 1. These samples yield Re–Os isotopic model ages ranging from 215.8 ± 5.8 Ma to 232.3 ± 4.0 Ma and a weighted average age of 225.0 ± 7.6 (Table 1, MSWD = 0.45, Fig. 3).

Samples								K-feldspar						
	DSG-2	DSG-3	DSG-4	TY-1	TY-2	TY-3	TY-4	YT-03	DSG-02	DSG-05	SJW-02	SJW-03	SJW-05	SJW-07
Rb	0.36	0.26	0.34	0.20	0.25	0.28	0.35	192	196	196	332	251	344	410
Ba	259	227	239	382	4937	1521	349	663	503	834	3950	2270	3540	2920
Th	0.35	0.04	0.13	0.12	0.10	0.09	0.15	0.98	0.05	0.11	0.57	0.27	0.25	0.21
U	0.45	0.54	0.44	6.55	4.28	6.24	3.96	1.59	0.73	1.06	0.87	0.32	6.43	3.04
Nb	0.37	0.50	0.33	0.07	0.11	0.08	0.05	5.22	1.81	1.94	1.28	0.52	1.92	0.10
Ta	0.13	0.10	0.15	0.09	0.07	0.13	0.12	0.04	0.02	0.02	0.05	0.09	0.09	0.05
Mo	2.72	0.69	13.4	11.4	6.82	3.52	5.62	325	3.80	7.92	78	93	455	10.5
La	165	102	101	95.0	127	87.0	112	33.7	1.62	8.62	8.99	4.94	5.78	3.80
Ce	443	304	271	185	202	149	218	46.2	2.42	13.50	13.7	6.26	5.78	4.78
Pb	113	95.0	68.0	62.0	46.0	70.0	62.0	40.0	140	81.4	55.8	52.4	57.0	84.4
Pr	61.2	45.2	38.8	24.1	24.1	18.6	27.1	4.62	0.25	1.75	1.80	0.60	0.62	0.60
Sr	5967	5182	4805	2610	1948	1588	2551	181	137	335	906	923	892	2140
Nd	290	221	192	112	107	86.0	122	14.0	1.00	7.23	7.15	1.98	2.18	2.34
Sm	80.7	65.7	57.5	33.7	29.3	24.8	36.2	1.46	0.25	1.69	1.18	0.26	0.38	0.46
Zr	0.63	0.27	0.38	0.33	0.60	0.25	0.48	1.68	0.14	2.06	1.29	8.67	3.89	1.12
Hf	0.80	0.63	1.03	0.66	0.47	0.32	0.60	0.03	0.004	0.09	0.05	0.23	0.08	0.02
Eu	26.2	21.4	18.8	11.8	10.9	9.40	12.2	0.61	0.03	0.71	2.30	1.22	1.95	1.68
Gd	104	85.4	82.5	50.4	38.6	34.4	51.0	1.89	0.15	1.81	1.34	0.34	0.41	0.45
Tb	14.9	12.5	11.0	6.70	5.00	4.40	7.20	0.13	0.04	0.29	0.14	0.03	0.06	0.08
Dy	102	85.3	73.2	44.4	31.6	28.3	46.4	0.36	0.22	1.44	0.56	0.10	0.28	0.35
Y	716	583	589	347	241	214	357	1.94	1.58	9.95	2.61	0.53	1.65	2.79
Ho	23.4	19.7	16.9	9.80	6.90	6.00	10.2	0.08	0.05	0.35	0.09	0.02	0.06	0.08
Er	76.8	64.5	55.4	31.8	21.6	19.6	32.7	0.29	0.18	1.12	0.32	0.07	0.20	0.27
Tm	12.9	11.1	9.59	5.41	3.64	3.24	5.60	0.03	0.05	0.18	0.03	0.01	0.03	0.04
Yb	92.3	79.1	68.1	38.8	26.2	22.9	40.4	0.19	0.21	1.25	0.14	0.06	0.21	0.28
Lu	13.9	11.8	9.94	5.60	3.73	3.30	5.82	0.04	0.04	0.19	0.02	0.01	0.04	0.04

4.2. Oxygen isotope

The oxygen isotopic composition of quartz separates from the Yuantou and Dashigou carbonatites (Table 2) has small variations ranging from 8.1‰ to 10.2‰ and with an average value of 9.1‰, which is consistent with average $\delta^{18}O$ composition (9‰) of quartz from igneous rocks (Blatt, 1987). Oxygen isotope of calcites from Yuantou and Dashigou orefields analyzed by Xu et al. (2010) range from 7.22 to 9.19‰.

4.3. Trace elements

The Re–Os dating results show that the molybdenites from Yuantou deposit have high Re content ranging from 159 to 301 ppm, which is consistent with that from the Dashigou carbonatites (278–289 ppm; Stein et al., 1997). The Re abundance of molybdenite from Shijiawan and other granite porphyries nearby are quite low (<100 ppm, Mao et al., 2008).

The ICP-MS analytical results of carbonatite whole rocks, K-feldspar and quartz mineral separates from carbonatites and granite porphyry are given in Table 3. The carbonatites from Yuantou, Wengongling, Dashigou, Taoyuan are enriched in all the trace elements except for Rb, Nb and Zr on the primary mantle-normalized abundance diagrams (Fig. 4a). They show peaks for Ba and U. It is noted that the rocks are characterized by markedly lower Th, Nb, Zr and higher heavy REE (HREE) contents relative to average calciocarbonatite worldwide (Hornig-Kjarsgaard, 1998; Woolley and Kempe, 1989). Chondrite normalized REE patterns for the carbonatites are light REE (LREE) slightly enriched but dominantly flat patterns with La/Yb_{CN} ratios ranging from 0.7 to 5.8. Ce and Eu anomalies are not observed in these rocks (Fig. 5a–d). This REE pattern is quite different from typical steep LREE-enrichment ($La/Yb_{CN} > 20$) of most carbonatites worldwide (Nelson et al., 1988; Woolley and Kempe, 1989 and references therein) and sulfide-bearing carbonatites from Phalaborwa ($La/Yb_{CN} = 74$–141, Hornig-Kjarsgaard, 1998).

The carbonatites from the above four deposits can be distinguished by Wengongling rock containing higher LREE abundance and absent

Pb anomaly, and Taoyan sample showing higher Ba, U and lower Th, Nb, REE compositions. Slight LREE enrichment is shown in the Wengongling samples ($La/Yb_{CN} = 3.8$–5.8). Xu et al. (2010) suggested that the carbonatites from Shijiawan have consistent positive Ba, U, Pb anomalies and negative Zr anomaly. They show high HREE content and relatively flat REE distribution pattern. Combined with 2 Yuantou, 12 Dashigou and 3 Shijiawan samples from Xu et al. (2010), the Nb/Ta and Zr/Hf ratios from Yuantou, Wengongling, Dashigou, Shijiawan, Taoyuan carbonatites have average values of 3.3, 6.4, 17, 10.3, 0.9 and 0.3, 0.5, 0.4, 0.1, 0.8, respectively, which are significantly lower than the average carbonatite worldwide (35, 60; Chakhmouradian, 2006) and primary mantle (18, 37; McDonough and Sun, 1995) values. However, the carbonatite Y/Ho ratio (32, 29, 29, 31, 35 from the above five locations) is similar and slightly higher than primary mantle value (28; McDonough and Sun, 1995).

Potassium-feldspar from the carbonatite and granite porphyry has consistent positive U and Pb anomalies in Fig. 4b. The K-feldspar from carbonatites can be distinguished by lower Rb, Ba, Th, U, Ta, Sr, Zr, Hf and higher REE (except of Eu) contents than that from granite porphyry. To be specific, average values of the Nb/Ta, Zr/Hf, Ba/Rb and Sr/Rb of the K-feldspar in carbonatites are 95, 38, 3.4 and 1.1, relative to values of 14, 37, 8.9 and 3.2, respectively, from porphyry deposit. Three K-feldspar samples from carbonatites show La/Yb_{CN} values 127, 5.6 and 4.9, respectively, and porphyry K-feldspars had La/Yb_{CN} values all above 10 with an average of 36. The maximum value of 127 may be probably due to the existence of LREE-rich mineral inclusion in the K-feldspar from carbonatites. It appears that higher level of LREE enrichment relative to HREE is shown in K-feldspar from the granite porphyry (Fig. 5e). The most significant distinction is that K-feldspar from the carbonatites shows slightly negative and negligible positive Eu anomaly ($\delta Eu = 0.5$–1.2), different from the obvious positive values ($\delta Eu = 2.4$–15) from granite porphyry.

Quartz from the carbonatite and granite porphyry has low trace element concentrations, most of which are 10 times lower than primary mantle values in Fig. 4c. The mineral shows consistent Nb, Pb, Zr and Hf negative anomalies. Geochemical differences have been observed in quartz from two rock types. Quartz from the carbonatites contains

Table 3 (continued)

Samples	Quartz									
	YT-03-1	YT-06	DSG-03	DSG-05-1	DSG-06	SJW-01	SJW-02-1	SJW-04	SJW-05-2	SJW-05-3
Rb	11.36	0.19	0.31	0.18	0.34	1.05	0.87	0.53	0.22	1.28
Ba	322	162	205	349	140	75.5	33.2	37.1	40.9	52.8
Th	0.39	0.44	0.30	0.79	0.10	0.70	0.22	0.11	0.18	0.33
U	1.49	0.08	0.46	0.14	0.11	0.20	0.06	0.07	0.05	0.06
Nb	2.37	0.11	0.55	0.28	0.36	0.05	0.12	0.08	0.18	0.43
Ta	0.03	0.03	0.01	0.18	0.03	0.001	0.06	0.01	0.26	0.02
Mo	7.55	1.32	10.7	2.76	14.5	3.75	13.5	5.47	31	38
La	21.0	26.8	17.3	36.8	4.70	36.0	8.54	4.31	6.29	15.6
Ce	30.0	36.9	25.5	48.0	7.17	46.5	11.2	5.62	8.70	20.7
Pb	36.4	5.70	14.7	10.6	21.6	10.6	8.97	8.20	10.5	4.12
Pr	2.70	3.07	2.21	3.88	0.68	3.73	0.86	0.44	0.69	1.68
Sr	216	110	332	280	70.8	59.0	32.4	31.1	36.4	54.7
Nd	8.82	9.62	7.07	11.3	2.28	10.4	2.35	1.26	1.95	5.04
Sm	1.08	0.91	0.75	0.84	0.33	0.69	0.21	0.09	0.17	0.35
Zr	3.94	0.09	0.23	0.15	2.24	0.13	0.24	0.14	0.30	0.85
Hf	0.10	0.01	0.01	0.01	0.05	0.001	0.002	0.01	0.01	0.01
Eu	0.23	0.16	0.14	0.14	0.10	0.10	0.04	0.02	0.02	0.06
Gd	0.68	0.50	0.33	0.29	0.20	bdl	bdl	0.03	bdl	0.05
Tb	0.11	0.08	0.06	0.07	0.05	0.04	0.02	0.01	0.01	0.02
Dy	0.49	0.26	0.25	0.25	0.17	0.05	0.05	0.02	0.02	0.05
Y	3.15	1.60	1.83	1.16	1.60	0.29	0.35	0.13	0.14	0.29
Ho	0.10	0.05	0.05	0.04	0.05	0.01	0.01	0.005	0.005	0.01
Er	0.35	0.20	0.20	0.15	0.17	0.07	0.03	0.01	0.02	0.06
Tm	0.05	0.02	0.03	0.02	0.03	0.002	0.004	0.001	0.003	0.004
Yb	0.40	0.18	0.21	0.14	0.17	0.02	0.03	0.01	0.005	0.03
Lu	0.07	0.03	0.03	0.02	0.03	0.003	0.005	0.001	0.003	0.003

somewhat higher abundance in every element except for Rb and Ta and positive Ba and U anomalies in Fig. 4c. Nb/Ta, Zr/Hf, Ba/Rb and Sr/Rb values of the quartz in carbonatite and porphyry deposits are 30, 29, 834, 724 and 12, 79, 81, 72, respectively. Chondrite normalized REE patterns for both of the quartz samples are LREE enriched without Ce and Eu anomalies, but those from carbonatites have higher HREE content and lower fractional level between LREE and HREE (La/Yb_{CN} = 20–86) than that (La/Yb_{CN} = 201–1197) from granite porphyry (Fig. 5f).

5. Discussion

The carbonatites from Huanglongpu occur as dykes, and are composed of mainly coarse, generally euhedral calcite grains. They are characterized by high Sr and REE contents, mantle-derived $\delta^{13}C_{PDB}$ and $\delta^{18}O_{SMOW}$ values, similar to carbonatites worldwide (Huang et al., 1994; Xu et al., 2007, 2010). It is indisputable that the Huanglongpu carbonatites are of typical mantle igneous origin.

The Yuantou deposit in Huanglongpu occurs in Archean gneiss, different from other deposits in the region of Huanglonpu such as Dashigou which occur in Mesoproterozoic volcanic and sediment rocks. Molybdenite from the Yuantou carbonatite deposit contains high Re contents (>150 ppm) and yields a Re–Os age of 225 Ma, which is consistent with that from Dashigou carbonatite deposit (221 Ma, Stein et al., 1997), but molybdenite from other porphyry or porphyry–skarn type Mo deposits, formed during Late Jurassic to Early Cretaceous (148~138 Ma), in Qinling region contains quite low Re content (several ppm; Mao et al., 2008). It was suggested by Mao et al. (1999) and Stein et al. (1997), on the basis of statistical analysis, the formation of the Mo-bearing deposits dominated by mantle-related process will give rise to the significantly higher Re abundance in molybdenite. Carbonatites from Yuantou and the other deposits show consistent trace element patterns, especially with high HREE content and slight fractionation between LREE and HREE (Fig. 5a–d). This indicates that all the carbonatite deposits of the Huanglongpu area, despite intruding distinct host rocks, were derived at the same time and from the same mantle source.

Notably that the carbonatites have abundant K-feldspar and quartz. Both minerals are also very common in the Mo-bearing veins in granite porphyry at Shijiawan or other porphyry Mo deposits. They have been considered as xenocrysts (Barker, 2001) or addition of the exotic components (Moore et al., 2009), rather than primary phases precipitated from carbonatitic magmas. This seems not to be the case in the Huanglongpu carbonatites, because (1) microscopic observation shows that K-feldspar and quartz in the carbonatites usually occur as euhedral phenocryst and mass aggregates (Fig. 2), respectively, in a fine-grained matrix of calcite. There are no overprint or reaction rims developed would indicate an origin as xenocrysts or by magma mixing (Barker, 2001; Moore et al., 2009); (2) the limited mantle-derived C and O isotope values ($\delta^{13}C$: −6.36 to −6.9‰, $\delta^{18}O$: 7.22 to 9.19‰; Xu et al., 2010) of carbonatites excluded the mixing or contamination with crustal components; (3) the carbonatite age is older than the Late Jurassic–Early Cretaceous granite porphyry in Huanglongpu (Zhao et al., 2010a, b). Both feldspar and quartz in the carbonatites cannot be captured from younger grantoids. Significant differences in the trace element patterns (Nb/Ta, Zr/Hf, Ba/Rb Sr/Rb and La/Yb_{CN}) of both minerals from carbonatites and granite porphyry are shown in Figs. 4b, c and 5e, f.

The K-feldspar from carbonatite shows slightly negative to negligible posititve Eu anomaly (δEu = 0.5–1.2), different from granite porphyry with a strongly positive Eu anomaly (δEu = 2.4–15). Europium is more compatible than other REE in feldspars precipitated from silicate magmas (White et al., 2003). However, this Eu anomaly of feldspar in the carbonatites cannot be explained by intense fractionation of primary feldspars because negative Eu anomaly is not observed in the whole rocks and their corresponding calcite and quartz. A possible explanation is that the carbonatitic magmas are characterized by the unusually high oxygen fugacites (indicated by the widespread presence of SO_4^{2-} with barite and sulfide assemblages), which will convert Eu^{2+} to Eu^{3+}. The K-feldspars in carbonatites cannot have positive Eu anomaly because Eu^{3+} is less compatible than Eu^{2+} in K-feldspar (Larsen, 2002). The quartz from carbonatites has lower values of La/Yb_{CN} (20–86), quite different from that in porphyry deposit (La/Yb_{CN} = 201–1197). The mineral has similar O isotopic composition (8.1–10.2‰) to the contemporaneous calcite (7.2–9.5‰). Fluid inclusions in quartz from the
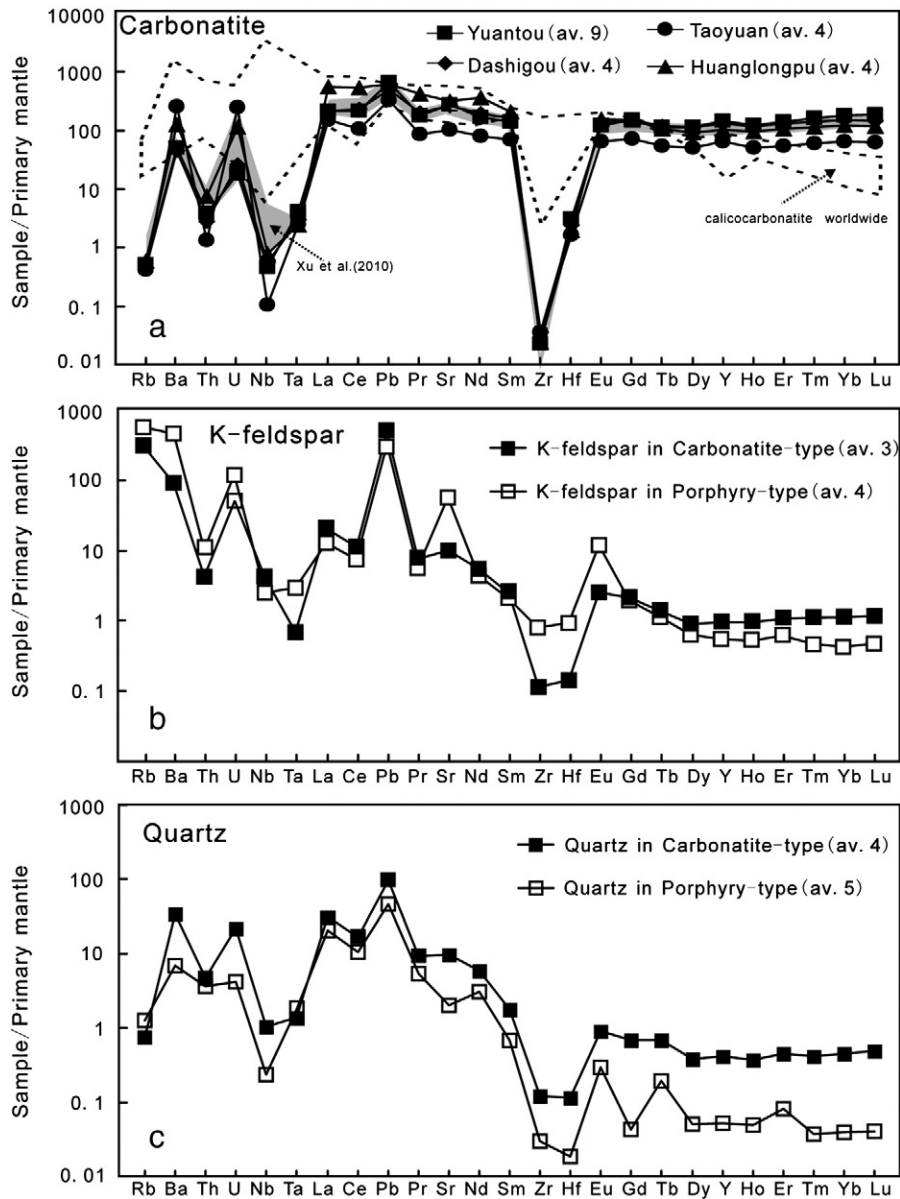
Fig. 4. Primitive mantle-normalized trace-element abundances of carbonatites, K-feldspar, quartz from carbonatites and granite porphyry in Huanglongpu deposit. The shaded data from Huanglongpu carbonatites are from Xu et al. (2010). Carbonatites worldwide are from Woolley and Kempe (1989). Normalization values are from McDonough and Sun (1995).

carbonatites show coexisting calcite and sulfate daughter-minerals (Song et al., unpublished). In addition, the K-feldspar and quartz in carbonatites are closely associated with molybdenite, which has primitive-mantle values of Re/Mo (Xu et al., 2010). Therefore, K-feldspar and quartz in Huanglongpu carbonatites, as well as molybdenite, are interpreted as primary mineral phases in carbonatites, rather than accidental xenocrysts.

There are several principal hypotheses for the origin of carbonatites: (1) direct melting of a carbonate-bearing mantle source (e.g., Harmer and Gitiins, 1998; Srivastava et al., 2005; Sweeney, 1994); (2) generation as immiscible liquids from CO_2-rich silicate magmas (e.g., Halama et al., 2005; Kjarsgaard and Hamilton, 1989; Koster van Groos and Wyllie, 1963); and (3) products of extensive crystal fractionation from a CO_2-rich silicate magma (e.g., Lee and Wyllie, 1994; Veksler et al., 1998a). Presently, the hypothesis that carbonatite magmas are generated by carbonate–silicate immiscibility has been mostly accepted due to the close association of carbonatite and alkaline silicate rocks (Barker, 1989). In the Huanglongpu area, field observation shows there are no contemporaneous silicate rocks spatially associated with the

carbonatites. As well as Late Jurassic granite porphyry in Shijiawan, a few alkaline granite porphyry and diabase dykes outcrop sporadically in the Huanglongpu area (Fig. 1). They have zircon U–Pb ages of 131 Ma and 129 Ma (Zhao et al., 2010b), respectively, which is younger than the carbonatites. It is proposed by recent experimental study that carbonatites produced by liquid immiscibility will be alkali-rich but with very low SiO_2 and Al_2O_3 contents (<1 wt.%) (Brooker and Kjarsgaard, 2011). Moreover, experiments designed by Jones et al. (1995) demonstrated that Mo will partition preferentially into the silicate liquid during carbonate and silicate melts immiscibility. These experimental results are opposite to the Huanglong carbonatites, which contain primary K-feldspar, quartz, and economic Mo concentrations. Thus, carbonate and silicate liquid immiscibility can not account for the origin of the Huanglongpu carbonatites.

Carbonatite magma is characterized by very low viscosity (Dobson et al., 1996), indicating the crystallization differentiation would play an important role in the evolution of the carbonatitic magmas. Xu et al. (2007) suggested that the Huanglongpu carbonatites are carbonate cumulates after fractionation and could not represent the primary
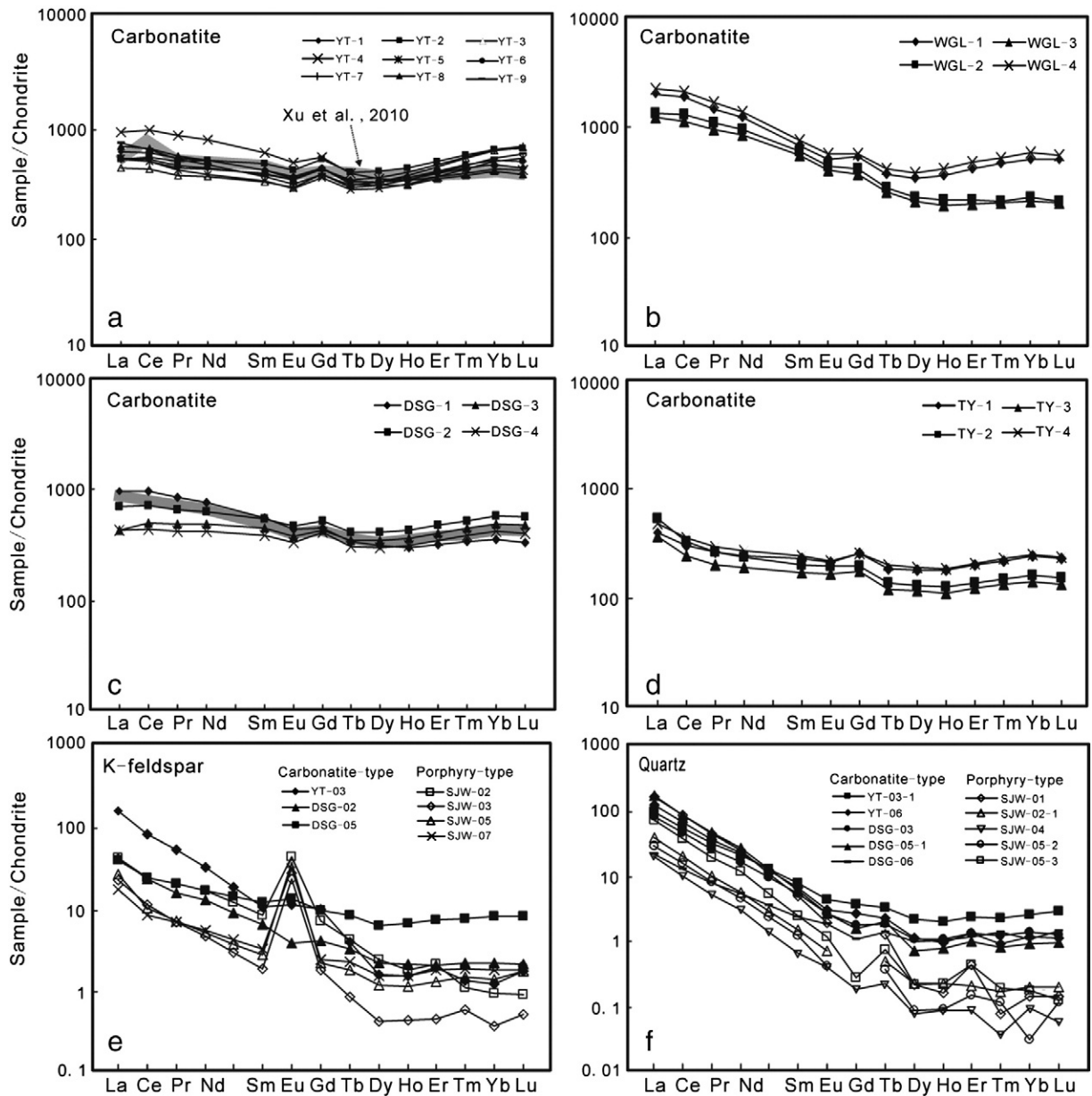
Fig. 5. Chondrite-normalized REE abundances of carbonatites, K-feldspar, quartz from carbonatites and granite porphyry in Yuantou (YT), Wengongling (WGL), Dashigou (DSG) and Taoyuan (TY). The shaded data are from Xu et al. (2010). Normalization values are from McDonough and Sun (1995).

magma, similar to most intrusive carbonatites (Woolley and Church, 2005). This conclusion can explain the geochemical features of the carbonatites in Huanglongpu. The rocks contain low Nb/Ta and Zr/Hf ratios, which may be attributed to fractionation of pyrochlore and titanite with high Nb/Ta and Zr/Hf (Chakhmouradian, 2006) and baddeleyite with high Zr/Hf (Chakhmouradian, 2006; Klemme and Meyer, 2003). Moreover, fractional crystallization of abundant non-silicate minerals, such as carbonates, oxides, and apatite, will increase the silica activity in the residual carbonatitic liquid (Barker, 2001; Rosatelli et al., 2003). Therefore, it is reasonable to postulate that Si, as well as Mo, due to their low crystal/melt partitioning coefficients, will have the incompatible behavior during the differentiation of carbonatitic magmas and be concentrated in the late liquid. Meanwhile, the extent of enrichment of these elements was further enhanced due to accumulation of voluminous calcite, finally leading to the generation of economic Mo mineralization and silicate minerals at Huanglongpu. Our results suggested that the carbonatitic magmas have the potential capacity of transporting and depositing metal sulfides, also as evidenced

from Phalaborwa where copper-bearing sulfides had been found in primary melt inclusions, suggesting the bornite mineralization was directly related to carbonatite magmatism (Palmer, 2001).

6. Conclusions

The Yuantou carbonatites intruding in Archean gneiss contain abundant molybdenite, which has consistent mineralization age with other carbonatite dykes in Mesoperoteroic volcanic and sediment rocks in the area, and is older than granite porphyry and associated Mo deposits in Qinling. These carbonatites in Huanglongpu have consistent REE distribution patterns with high HREE content and slight fractionation between LREE and HREE. K-feldspar and quartz, as well as molybdenite, are common and crystallized from the carbonatites. This indicates that the primary carbonatitic liquids are enriched in Si and Mo, which is related to strong fractional crystallization of carbonates and oxides.

765

Acknowledgments

References

Barker, D.S., 1989. Field relations of carbonatites. In: Bell, K. (Ed.), Carbonatites: Genesis and Evolution. Unwin Hyman, London, pp. 38–69.

Barker, D.S., 2001. Calculated silica activities in carbonatite liquids. Contrib. Mineral. Petrol. 141, 704–709.

Blatt, H., 1987. Oxygen isotopes and the origin of quartz. J. Sediment. Petrol. 57, 373–377.

Brooker, R.A., Kjarsgaard, B.A., 2011. Silicate–carbonate liquid immiscibility and phase relations in the system SiO_2–Na_2O–Al_2O_3–CaO–CO_2 at 0.1–2.5 GPa with applications to carbonatite genesis. J. Petrol. 52, 1281–1305.

Chakhmouradian, A.R., 2006. High-field-strength elements in carbonatitic rocks: geochemistry, crystal chemistry and significance for constraining the sources of carbonatites. Chem. Geol. 235, 138–160.

Dalton, J.A., Presnall, D.C., 1998. Carbonatitic melts along the solidus of model lherzolite in the system CaO–MgO–Al_2O_3–SiO_2–CO_2 from 3 to 7 GPa. Contrib. Mineral. Petrol. 131, 123–135.

Dobson, D.P., Jones, A.P., Rabe, R., Sekine, T., Kurita, K., Taniguchi, T., Kondo, T., Kato, T., Shimomura, O., Urakawa, S., 1996. In-situ measurement of viscosity and density of carbonate melts at high pressure. Earth Planet. Sci. Lett. 143, 207–215.

Eriksson, S.C., 1989. Phalabowra: a saga of magmatism, metasomatism and miscibility. In: Bell, K. (Ed.), Carbonatites: Genesis and Evolution. Unwin Hyman, London, pp. 221–254.

Gitins, J., Harmer, R.E., Barker, D.S., 2005. The bimodal composition of carbonatites: reality or misconception? Lithos 85, 129–139.

Halama, R., Vennemann, T., Siebel, W., Markl, G., 2005. The GrØnnedal-Ika carbonatite–syenite complex, South Greenland: carbonatite formation by liquid immiscibility. J. Petrol. 46, 191–217.

Harmer, R.E., Gitiins, J., 1998. The case for primary, mantle-derived carbonatite magma. J. Petrol. 39, 1895–1903.

Heinrich, E.W., 1970. The Palabora carbonatitic complex-a unique copper deposit. Can. Mineral. 10, 585–598.

Horgarth, D.D., 1989. Pyrocholre, apatite and amphibole: distinctive minerals in carbonatite. In: Bell, K. (Ed.), Carbonatites: Genesis and Evolution. Unwin Hyman, London, pp. 105–148.

Hornig-Kjarsgaard, I., 1998. Rare earth elements in sovitic carbonatites and their mineral phases. J. Petrol. 39, 2105–2121.

Huang, D.H., Wu, C.Y., Du, A.D., He, H.L., 1994. Re–Os isotope age of molybdenum deposits in East Qinling and their significance. Mineral Deposits 13, 221–230 (in Chinese with English abstract).

Jones, J.H., Walker, D., Pickett, D.A., Murrell, M.T., Beattie, P., 1995. Experimental investigations of the partitioning of Nb, Mo, Ba, Ce, Pb, Ra, Th, Pa, and U between immiscible carbonate and silicate liquids. Geochim. Cosmochim. Acta 59, 1307–1320.

Kjarsgaard, B.A., Hamilton, D.L., 1989. The genesis of carbonatites by immiscibility. In: Bell, K. (Ed.), Carbonatites: Genesis and Evolution. Unwin Hyman, London, pp. 388–404.

Klemme, S., Meyer, H.P., 2003. Trace elements partitioning between baddeleyite and carbonatite melt at high pressures and high temperatures. Chem. Geol. 199, 233–242.

Korobeinikov, A.N., Mitrofanov, F.P., Gehör, S., Laajoki, K., Pavlov, V.P., Mamontov, V.P., 1998. Geology and copper sulphide mineralization of the Salmagorskii ring igneous complex, Kola Peninsula, NW Russia. J. Petrol. 39, 2033–2041.

Koster van Groos, A.F., Wyllie, P.J., 1963. Experimental data bearing on the role of liquid immiscibility in the genesis of carbonatites. Nature 199, 801–802.

Kröner, A., Compston, W., Zhang, G.W., Guo, A.L., Todt, W., 1988. Age and tectonic setting of Late Archean greenstone-gneiss terrain in Henan Province, China, as revealed by single-grain zircon dating. Geology 16, 211–215.

Larsen, R.B., 2002. The distribution of rare-earth elements in K-feldspar as an indicator of petrogenetic processes in granitic pegmatites: examples from two pegmatite fields in southern Norway. Can. Mineral. 40, 137–152.

Le Bas, M.J., 1989. Diversification of carbonatite. In: Bell, K. (Ed.), Carbonatites: Genesis and Evolution. Unwin Hyman, London, pp. 428–447.

Le Maitre, R.W., 2002. Igneous Rocks: A Classification and Glossary of Terms. Cambridge University Press, Cambridge.

Lee, W.J., Wyllie, P.J., 1994. Experimental data bearing on liquid immiscibility, crystal fractionation, and the origin of calciocarbonatites and natrocarbonatites. Int. Geol. Rev. 36, 797–819.

Li, N., Chen, Y.J., Zhang, H., Zhao, T.P., Deng, X.H., Wang, Y., Ni, Z.Y., 2007. Molybdenum deposits in East Qinling. Earth Sci. Front. 14, 186–198 (in Chinese with English Abstract).

Lindner, M., Leich, D.A., Russ, G.P., Bazan, J.M., Borg, R.J., 1989. Direct determination of the half-life of ^{187}Re. Geochim. Cosmochim. Acta 53, 1597–1606.

Mao, J.W., Zhang, Z.C., Zhang, Z.H., Du, A.D., 1999. Re–Os isotopic dating of molybdenites in the Xiaoliugou W–(Mo) deposit in the northern Qulian Mountains and its geological significance. Geochim. Cosmochim. Acta 63, 1815–1818.

Mao, J.W., Xie, G.Q., Bierlein, F., Qu, W.J., Du, A.D., Ye, H.S., Pirajno, F., Li, H.M., Guo, B.J., Lie, Y.F., Yang, Z.Q., 2008. Tectonic implications from Re–Os dating of Mesozoic molybdenum deposits in the East Qinling–Dabie orogenic belt. Geochim. Cosmochim. Acta 72, 4607–4626.

Mariano, A.N., 1989. Nature of economic mineralization in carbonatites and related rocks. In: Bell, K. (Ed.), Carbonatites: Genesis and Evolution. Unwin Hyman, London, pp. 149–175.

Mattauer, M., Matte, P., Tapponier, P., 1985. Tectonics of the Qinling belt: build-up and evolution of eastern Asia. Nature 317, 496–500.

McDonough, W.F., Sun, S.S., 1995. The composition of the Earth. Chem. Geol. 120, 223–253.

Meng, Q.R., Zhang, G.W., 2000. Geologic framework and tectonic evolution of the Qinling orogen, central China. Tectonophysics 323, 183–196.

Moore, K.R., Wall, F., Divaev, F.K., Savatenkov, V.M., 2009. Mingling of carbonate and silicate magmas under turbulent flow conditions: evidence from rock textures and mineral chemistry in subvolcanic carbonatite dykes, Chagatai, Uzbekistan. Lithos 110, 65–82.

Nelson, D.R., Chivas, A.R., Chappell, B.W., McCulloch, M.T., 1988. Geochemical and isotopic systematics in carbonatites and implications for the evolution of ocean-island sources. Geochim. Cosmochim. Acta 52, 1–17.

No.13 Geological Team Shanxi Geological Bureau, 1989. The detailed geological report of Huanglongpu Mo ore area in Luona, Shanxi Province. Geological Report of Shanxi Province (in Chinese).

Palabora Mining Company, 1976. The geology and the economic deposits of copper, iron, and vermiculite in the Palabora igneous complex: a brief review. Econ. Geol. 71, 177–192.

Palmer, D.A.S., 2001. The Evolution of Carbonatite Melts and their Aqueous Fluids: Evidence from Amba Dongar, India, and Phalaborwa, South Africa. 2001. Ph.D. Thesis McGill University (339 pp.).

Qi, L., Hu, J., Gregoire, D.C., 2000. Determination of trace elements in granites by inductively coupled plasma mass spectrometry. Talanta 51, 507–513.

Qi, L., Zhou, M.F., Gao, J.F., Zhao, Z., 2010. An improved Carius tube technique for determination of low concentrations of Re and Os in pyrites. J. Anal. At. Spectrom. 25, 585–589.

Ratschbacher, L., Hacker, B.R., Calvert, A., Webb, L.E., Grimmer, J.C., McWilliams, M.O., Ireland, T., Dong, S.W., Hu, J.M., 2003. Tectonic of the Qinling (Central China): tectonostratigraphy, geochronology, and deformation history. Tectonophysics 366, 1–53.

Rosatelli, G., Wall, F., Le Bas, M.J., 2003. Potassic glass and calcite carbonatite in lapilli from extrusive carbonatites at Rangwa Caldera Complex, Kenya. Mineral. Mag. 67, 931–955.

Rudashevsky, N.S., Kretser, Y.U.L, Bulakh, A.G., Rudashevsky, V.N., 2001. Two types of PGE mineralisations in carbonatite deposits (Phalaborwa Massif, South Africa and Kovdor Massif, Russia). J. Afr. Earth Sci. 32 (1), A30.

Srivastava, R.K., Heaman, L.M., Sinha, A.K., Sun, S.H., 2005. Emplacement age and isotope geochemistry of Sung Valley alkaline–carbonatite complex, Shillong Plateau, northeastern India: implications for primary carbonate melt and genesis of the associated silicate rocks. Lithos 81, 33–54.

Stein, H.J., Markey, R.J., Morgan, M.J., Du, A., Sun, Y., 1997. Highly precise and accurate Re–Os ages for molybdenite from the East Qinling–Dabie molybdenum belt, Shaanxi province, China. Econ. Geol. 92, 827–835.

Sun, W.D., Li, S.G., Chen, Y.D., Li, Y.J., 2000. Zircon U–Pb dating of granitoids from South Qinling, Central China and their geological significance. Geochimica 29, 209–216 (in Chinese with English Abstract).

Sun, W.D., Li, S.G., Sun, Y., Zhang, G.W., Li, Q.L., 2002. Mid-Paleozoic collision in the north Qinling: Sm–Nd, Rb–Sr and $^{40}Ar/^{39}Ar$ ages and their tectonic implications. J. Asian Earth Sci. 21, 69–76.

Sweeney, R., 1994. Carbonatite melt compositions in the earth mantle. Earth Planet. Sci. Lett. 128, 259–270.

Veksler, I.V., Nielsen, T.F.D., Sokolov, S.V., 1998. Mineralogy of crystallized melt inclusions from Gardiner and Kovdor ultramafic alkaline complexes: implications for carbonatite genesis. J. Petrol. 39, 2015–2031.

Wallace, M.E., Green, D.H., 1988. An experimental determination of primary carbonatite magma composition. Nature 335, 343–346.

White, J.C., Holt, G.S., Parker, D.F., Ren, M., 2003. Trace-element partitioning between alkali feldspar and peralkalic quartz trachyte to rhyolite magma. Part I: Systematics of trace-element partitioning. Am. Mineral. 88, 316–329.

Woolley, A.R., Church, A.A., 2005. Extrusive carbonatites: a brief review. Lithos 85, 1–14.

Woolley, A.R., Kempe, D.R.C., 1989. Carbonatites: nomenclature, average chemical composition. In: Bell, K. (Ed.), Carbonatites: Genesis and Evolution. Unwin Hyman, London, pp. 1–14.

Xu, C., Campbell, I.H., Allen, C.M., Huang, Z.L., Qi, L., Zhang, H., Zhang, G.S., 2007. Flat rare earth element patterns as an indicator of cumulate processes in the Lesser Qinling carbonatites, China. Lithos 95, 267–278.

Xu, C., Campbell, I.H., Kynicky, J., Allen, C.M., Chen, Y.J., Huang, Z.L., Qi, L., 2008. Comparison of the Daluxiang and Maoniuping carbonatitic REE deposits with Bayan Obo REE deposits, China. Lithos 106, 12–24.

Xu, C., Kynicky, J., Chakhmouradian, A.N., Qi, L., Song, W.L., 2010. A unique Mo deposit associated with carbonatites in the Qinling orogenic belt, central China. Lithos 118, 50–60.

Xu, C., Taylor, R.N., Kynicky, J., Chakhmouradian, A.R., Song, W.L., Wang, L.J., 2011. The origin of enriched mantle beneath North China block: evidence from young carbonatites. Lithos 127, 1–9.

Zhao, H.J., Mao, J.W., Ye, H.S., Hou, K.J., Liang, H.S., 2010a. Geochronology and petrogenesis of Shijiawan granite porphyry in Shaanxi Province: constraints from zircon U–Pb geochronology and Hf isotopic composition. Mineral Deposits 29, 143–157 (In Chinese with English Abstract).

Zhao, H.J., Mao, J.W., Ye, H.S., Xie, G.Q., Yang, Z.Q., 2010b. Geochronology and geochemistry of the alkaline granite porphyry and diabase dikes in the Huanglongpu area of Shaanxi Province: petrogenesis and their implications for tectonic environment. Geol. China 37, 12–27 (In Chinese with English Abstract).